TÜBİTAK

Turkish Journal of Chemistry

http://journals.tubitak.gov.tr/chem/

Research Article

Turk J Chem
(2016) 40: 117 – 124

doi:10.3906/kim-1502-95

Durability of carbon/conducting polymer composite supported Pt catalysts prepared by supercritical carbon dioxide deposition

Gamze BOZKURT[1], **Fulya MEMİOĞLU**[2], **Ayşe BAYRAKÇEKEN YURTCAN**[1,2,*]
[1]Department of Nanoscience and Nanoengineering, Faculty of Engineering, Atatürk University, Erzurum, Turkey
[2]Department of Chemical Engineering, Faculty of Engineering, Atatürk University, Erzurum, Turkey

Received: 18.02.2015 • **Accepted/Published Online:** 03.08.2015 • **Final Version:** 05.01.2016

Abstract: Polypyrrole (PPy)/carbon (C) composites were synthesized by oxidative chemical polymerization and used as support material for Pt nanoparticles. PPy/C supported Pt nanoparticles were prepared by using a promising catalyst preparation method, supercritical carbon dioxide ($scCO_2$) deposition. The prepared materials were characterized by using BET, TGA, XRD, and TEM techniques. Cyclic voltammetry was used in order to determine the electrocatalytic activity of the prepared catalyst for hydrogen oxidation and oxygen reduction reactions that occur in proton exchange membrane fuel cells (PEMFCs). The Pt loading obtained over the composite material was around 10%. TEM results showed highly dispersed and small nanoparticles over the composite material by using $scCO_2$ deposition. Pt dissolution/agglomeration and carbon corrosion tests were applied to the composite supported Pt catalyst in order to determine its durability.

Key words: Platinum nanoparticles, degradation, supercritical carbon dioxide deposition, polymer composites

1. Introduction

In recent years, conductive nanofiller/polymer composites have gained importance due to their outstanding properties.[1] Conductive polymers have different application fields including transducers, bio and chemical sensors, rechargeable batteries, antistatic coatings, and corrosion-inhibiting films.[2] The most commonly used polymers are polyacetylene, polypyrrole (PPy),[3] polyaniline, polythiophene,[4] and derivate for electrocatalytic applications.[5] Among these, PPy can be used as conducting filler in the preparation of electrically conducting composites[6] because of its great electrical conductivity and environmental stability.[7,8] In addition, PPy is a member of the conjugated polymer family, which have unique properties because their doping level can be readily controlled through an acid doping/base dedoping process.[9] PPy is used in many fields such as electronic devices, solid electrolytic capacitors, gas sensors, polymeric batteries, packaging, and microactuators. PPy can be synthesized by either oxidatively chemical or electrochemical polymerization of pyrrole.[10] PPy shows high stability and electronic and ionic conductivity, and reversible redox properties, and increases the activity of electrocatalysts. Therefore, PPy is used to obtain higher currents compared to polymer-free catalysts.[11] In particular, PPy is used to improve the electrocatalysis ability of Pt/carbon catalyst for fuel cell application.[9] Composites of PPy with carbonous materials can improve its electrical conductivity and will provide the requirements for energy materials and can be used as the support materials in catalysis.[12]

*Correspondence: ayse.bayrakceken@gmail.com

Supported materials are a major field in catalysis. There are many different catalyst preparation techniques aimed to synthesize catalysts with desired properties. One of the promising supported catalyst preparation methods is supercritical carbon dioxide ($scCO_2$) deposition, which utilizes the advantages of carbon dioxide's nontoxic and environmentally acceptable properties.[2] The $ScCO_2$ method includes the dissolution of an organometallic precursor in supercritical fluid and adsorption of dissolved precursor over the porous support. After adsorption of the precursor on the support, the precursor is converted to its metallic form via chemical or thermal reduction.[13]

Carbon-supported Pt catalysts are the most commonly used ones in proton exchange membrane fuel cells (PEMFCs). Particle size, structural effects, and dispersion are the important factors that influence electrocatalytic activity.[14] The most important problems with PEMFC catalysts are their high cost and lack of durability.[15,16] Many studies have attempted to improve the performance and durability of conventional catalysts. Some of those focused on the use of a bimetallic catalyst and alloys. However, when cheap transition metals are used they can dissolve and transfer to the polymer phase.[17]

In PEMFCs, platinum or its alloys supported by high surface carbon serve as cathode and anode electrodes. In a PEMFC, the kinetics at the cathode (oxygen reduction reaction (ORR)) is sluggish when compared to that at the anode (hydrogen oxidation reaction (HOR)). Therefore, the large overpotential, about 80% portion of the total cell voltage losses, comes from ORR.[14] Carbon corrosion also occurs during the long-term operations of the PEMFC, which results in performance losses due to carbon and Pt nanoparticle losses.[18] PPy/C supported Pt catalysts seem to be an alternative in order to decrease the performance losses in PEMFCs due to carbon corrosion.

In the present study, PPy/carbon composites were used as the support material for Pt nanoparticles. Pt nanoparticles were applied to this composite by using supercritical carbon dioxide ($scCO_2$) deposition. The prepared catalyst was characterized by using BET, XRD, TGA, and TEM and the electrochemical characterization was achieved by using cyclic voltammetry (CV).

2. Results and discussion

The nitrogen adsorption/desorption isotherm of the synthesized PPy/C composite is given in Figure 1. The multipoint BET surface area of the composite material was 77 m^2/g. The plain carbon surface area (250 m^2/g) decreased with the addition of PPy because of blockage of the pores of the carbon with PPy.[19]

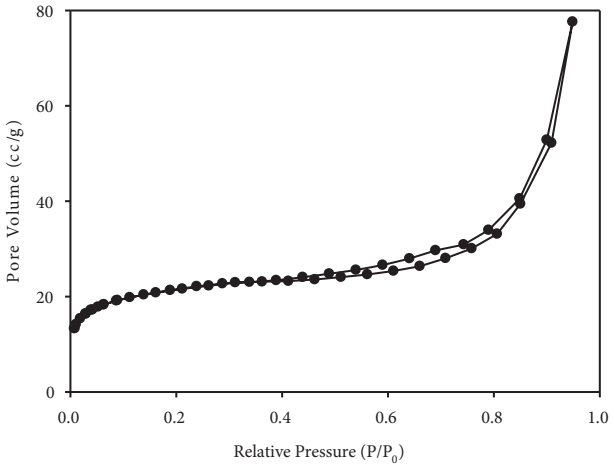

Figure 1. Nitrogen adsorption/desorption isotherms for the composite.

TGA was used to determine the Pt loading over the composite material. The TGA results for the plain composite and also the Pt loaded catalyst are given in Figure 2 and the Pt loading over the composite material was around 10%.

XRD patterns were used to determine the crystallinity of the prepared catalyst. The XRD patterns for the plain composite and the catalyst are given in Figure 3. The XRD pattern of the PPy/C composite showed an intermediary characteristic between the carbon and PPy.[12] Characteristic peaks of face-cubic-centered (fcc) Pt were obtained as (111), (200), and (220). There was an overlapping of the Pt (111) and (200) peaks with the carbon characteristic peak located at 43°.[12] The particle sizes of the Pt nanoparticles were calculated using the Scherrer equation by using the (220) plane. The particle sizes of the nanoparticles were approximately 1.6 nm. TEM images for the prepared catalyst are given in Figure 4. TEM results showed that highly dispersed and small and spherical nanoparticles can be obtained by the $scCO_2$ deposition method.

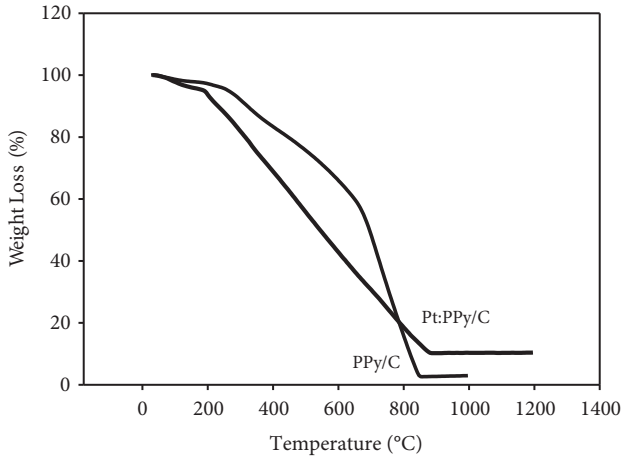

Figure 2. TGA results for the composite and the catalyst.

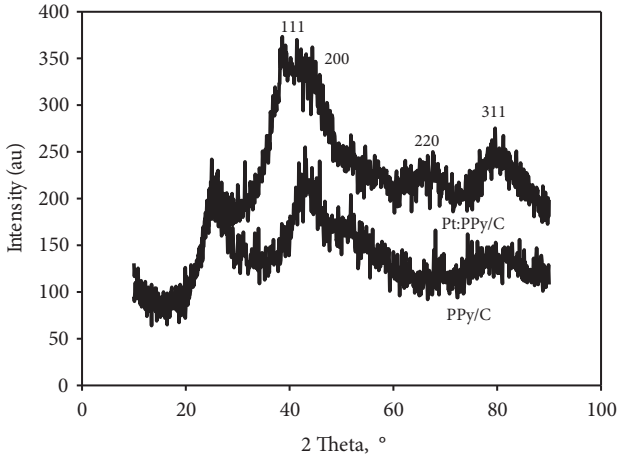

Figure 3. XRD patterns for the plain composite and the catalyst.

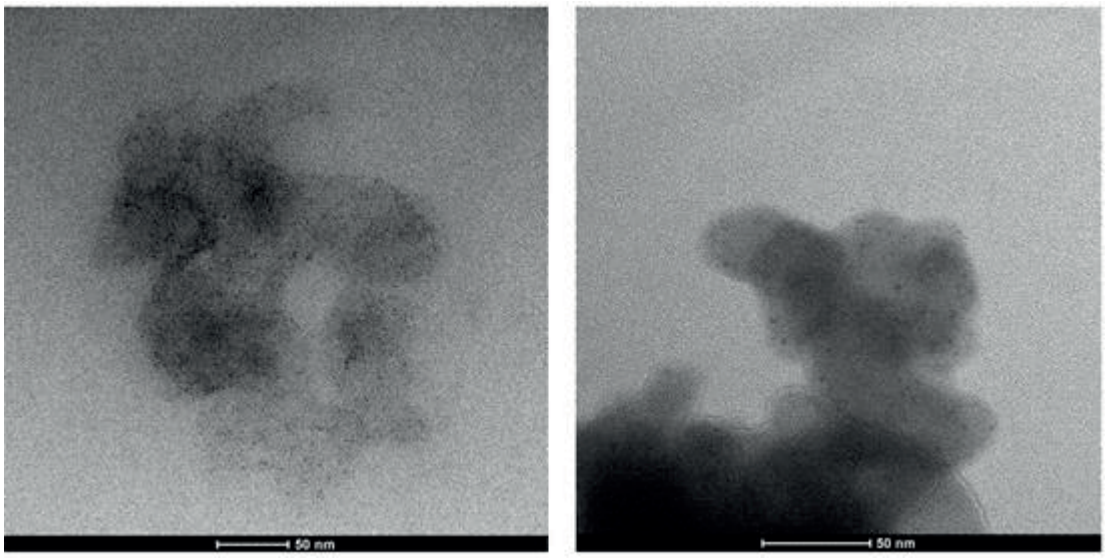

Figure 4. TEM images of the prepared catalyst.

Electrochemical characterization of the catalyst was performed using cyclic voltammetry. The corresponding cyclic voltammogram for HOR activity before and after the Pt degradation test is given in Figure 5. Electrochemical surface area (ESA) of the catalyst was calculated by taking into account the average of adsorption and desorption areas of the cyclic voltammograms. The change after the degradation tests was obtained by comparing the voltammograms before and after the degradation tests. ESA of the catalyst was decreased about 43% after the Pt dissolution/agglomeration test. There are different proposed mechanisms for Pt dissolution/agglomeration during long-term operations of the PEM fuel cell. Small Pt nanoparticles can migrate over the support material and agglomerate with other nanoparticles in order to decrease their surface energy. This phenomenon resulted in an increase in the particle size, which decreased the surface area. This mechanism is known as Ostwald ripening.[18] The decrease in the double layer capacitance also can be attributed to the decrease in the possible surface oxide groups and also the possible leaching of the dopant from the composite, which may cause instability of the composite material.[4] The obtained ESA of the catalyst in this study is smaller than those reported in the literature and this can be attributed to the lower surface area of the composite material when compared to a plain carbon support. ORR activity of the catalyst was also determined before and after the Pt dissolution/agglomeration procedure (Figure 6). Tafel slope losses before and after the degradation test are summarized in Table 1. As can be seen, an insignificant Tafel slope loss (0.96 mV) was obtained for the prepared catalyst after the Pt dissolution/agglomeration test.

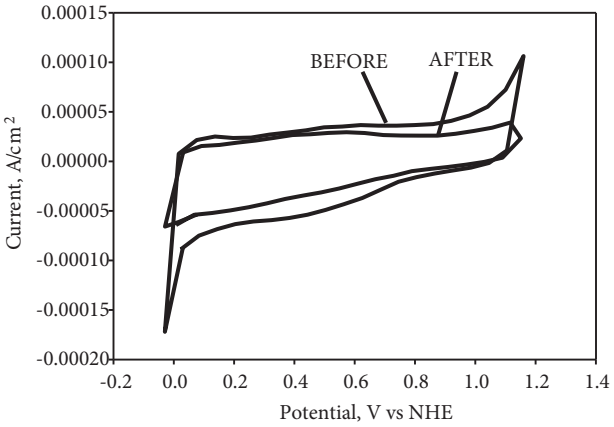

Figure 5. Cyclic voltammogram before and after Pt dissolution/agglomeration.

Table 1. ESA losses resulting from Pt dissolution/agglomeration and carbon corrosion tests.

Catalyst	Desorption area before degradation (m^2/g)	Adsorption area before degradation (m^2/g)	Desorption area before degradation (m^2/g)	Adsorptio area before degradation (m^2/g)	% Loss
		Carbon corrosion			
Pt-PPy/C	19.3	8.4	9.6	4.5	49.1
		Pt dissolution			
Pt-PPy/C	6.7	1.7	3.7	1.1	43.0

Carbon corrosion was another degradation test applied to the fresh electrode. HOR activity of the catalyst before and after carbon corrosion is given in Figure 7. ESA loss was calculated as 49% after carbon corrosion, which is slightly higher than the ESA loss after the Pt dissolution/agglomeration test. After the carbon corrosion

test between 0.4 and 0.6 V (vs. NHE) a clear peak was observed corresponding to the oxidation of carbon, which is thermodynamically favorable above 0.2 V. After the carbon corrosion test the double layer capacitance was higher, which can be attributed to the increase in surface oxide groups. ORR activity of the catalyst was also investigated before and after the carbon corrosion test. Hydrodynamic voltammograms of the prepared catalyst and Tafel slopes before and after carbon corrosion are given in Figure 8. From Table 2, it is seen that a 3.6 mV Tafel slope loss occurred after the carbon corrosion degradation test, which is higher than that obtained after the Pt dissolution/agglomeration test. Both Pt dissolution/agglomeration and carbon corrosion degradation test results showed that especially ESA loss is significant, which has to be improved further, but the Tafel slope losses were very small, which indicates that ORR activity did not decrease very much after degradation.

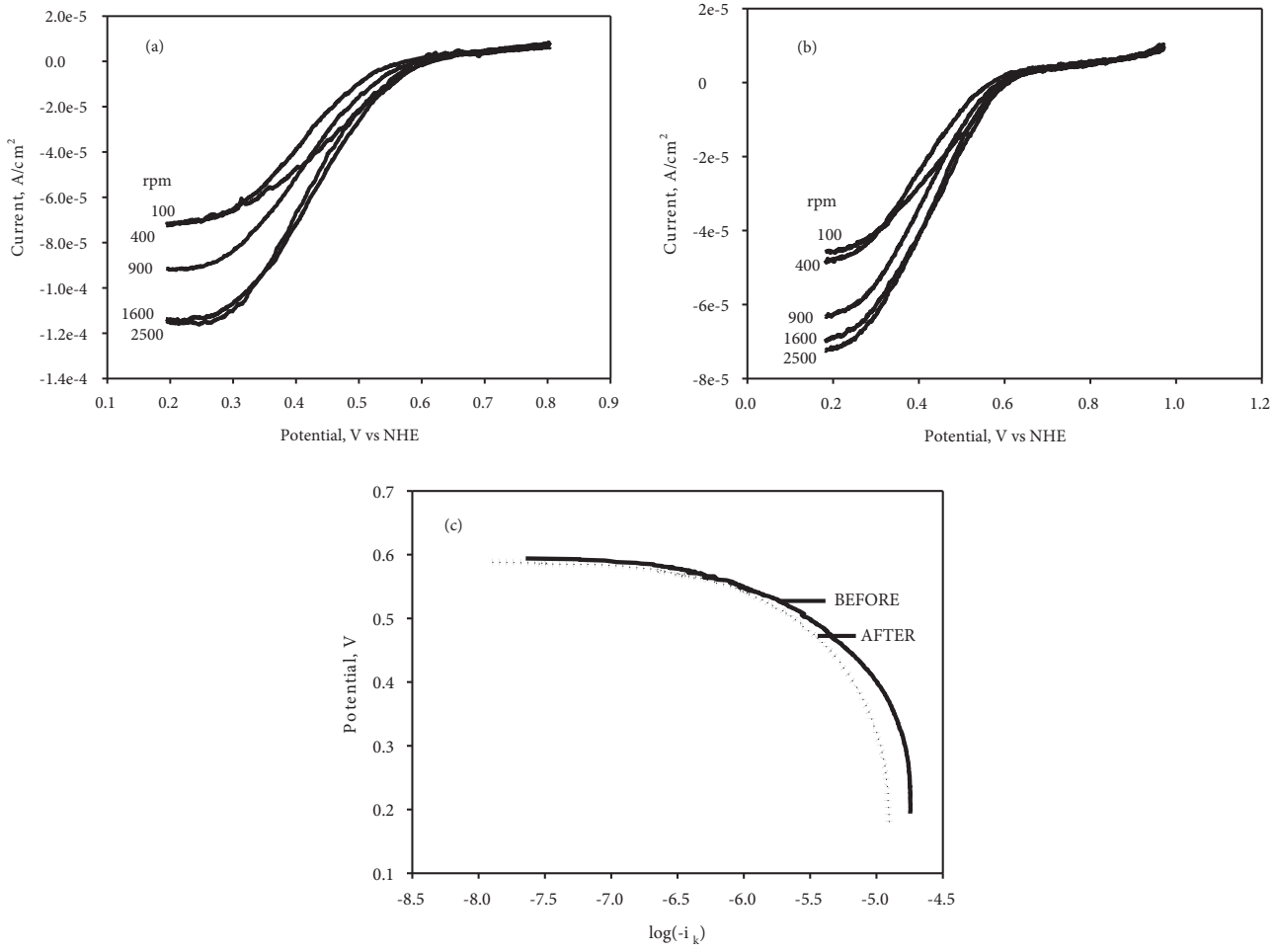

Figure 6. a) Hydrodynamic voltammograms before Pt degradation test; b) Hydrodynamic voltammograms after Pt degradation; c) Tafel slope.

The dispersion of the catalyst nanoparticles strongly depends on the properties of the support materials. The higher the surface area is the smaller the nanoparticles obtained. The results obtained in this study showed that although the surface area of the PPy/C composite decreased when compared to plain carbon, the $scCO_2$ deposition method provides a uniform dispersion of Pt nanoparticles having small particles sizes over the PPy/C composites.

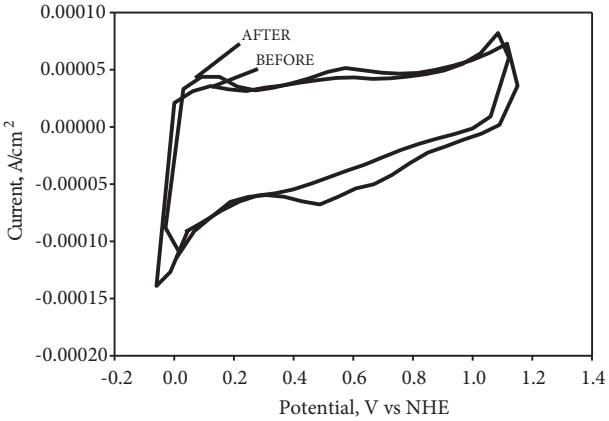

Figure 7. Cyclic voltammogram before and after carbon corrosion.

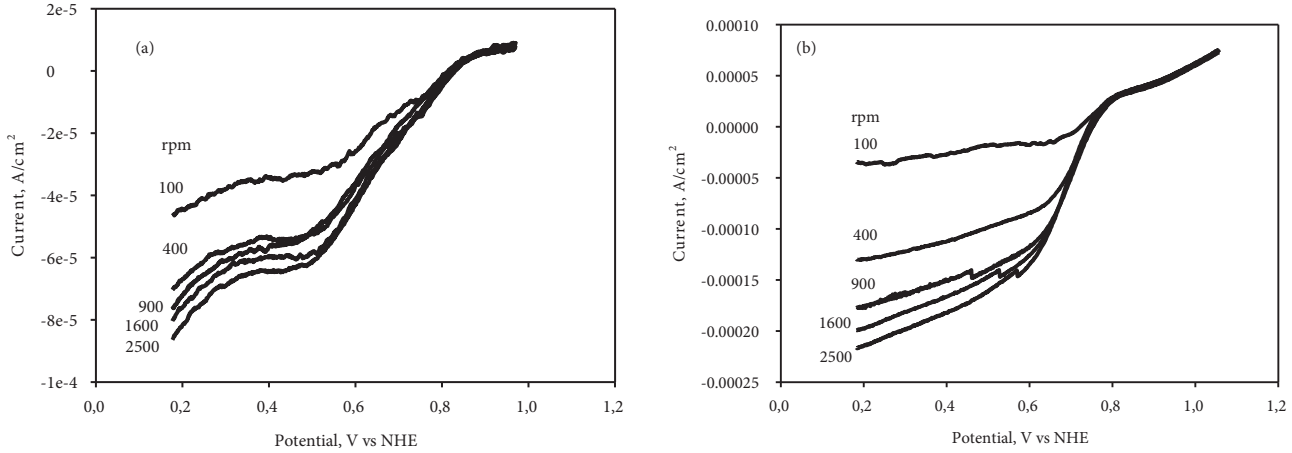

Figure 8. a) Hydrodynamic voltammograms before carbon corrosion; b) Hydrodynamic voltammograms after carbon corrosion; c) Tafel slope.

Table 2. Tafel slope losses after degradation tests.

Catalyst	% Pt	Tafel slope potential loss (mV)	% Tafel slope loss
Carbon corrosion			
Pt-PPy/C	10	3.60	2.40
Pt dissolution/agglomeration			
Pt-PPy/C	10	0.96	0.95

CV results also showed that the electrochemically active surface areas of the prepared catalyst were smaller than those reported in the literature. Further studies are needed in order to increase the ESA of the catalysts. PPy/C supported Pt nanoparticles were prepared using chemical reduction [20] by other authors. They found higher ESAs when compared to our study. The main differences were the Pt loading over the composite material and over the GC electrode and also the catalyst preparation method. In this study, we got 10% Pt loading whereas they obtained 40% Pt loading over the PPy/C composite. They also used 200 μgPt cm^{-2} while we used 28 μgPt cm^{-2} loading over the GC electrode during CV experiments. These differences may explain the different results obtained from the PPy/C supported Pt catalysts.

3. Experimental

Composite material was synthesized by in situ chemical oxidative polymerization of pyrrole over carbon support (C, Vulcan XC 72, Cabot).[12] C was firstly treated with nitric acid and then weighed and the required amount was mixed with ethanol for 30 min and then pyrrole monomer was dissolved in distilled water and added to this mixture. After another 30 min of stirring, the p-toluene sulfonic acid (p-TSA) dopant was added to this mixture. Ammonium persulfate solution used as the oxidant was added to this mixture and stirring continued for 24 h. This polymerization process was performed at 0 °C.

PPy/C supported Pt nanoparticles were obtained by using supercritical carbon dioxide ($scCO_2$) deposition. 1,5 Dimethyl platinum cyclooctadiene (Me_2PtCOD, Strem Chemicals) was used as the organometallic Pt precursor. The Pt precursor was firstly dissolved in $scCO_2$ (at 70 °C and 24 MPa) and then adsorbed on the composite material. The precursor was reduced to metallic Pt form with heat treatment at 200 °C for 4 h in nitrogen atmosphere.

The structural properties of the composite were determined with a surface area analyzer (Quantachrome Autosorb-1C and Micromeritics Gemini V 2365). Thermal behavior of the catalyst was studied in a Netzsch Thermal analyzer (TGA) in air atmosphere in order to determine the Pt loading over the composite material. The crystallinity of the prepared catalyst was determined by using a Rigaku Miniflex X-ray diffractometer (XRD) CuKα ($\lambda = 1.5406$ Å). Transmission electron microscope (TEM) analysis was carried out with a JEOL JEM 2100F STEM instrument.

The electrochemical characterization of the prepared catalyst was performed using CV scans by the procedure given elsewhere.[18] The CV setup was purchased from Pine Instruments and connected to a Versastat 3 potentiostat. CV analyses were carried out in a standard three-electrode electrochemical cell configuration. Briefly, catalyst ink was prepared by mixing measured amounts of the prepared catalysts with deionized water, 1,2-propanediol, and 15% Nafion solution. The suspension was ultrasonicated for 1 h. The required amount of catalyst to prepare a 5-mm diameter glassy carbon (GC) electrode with a Pt loading of 28 μgPt cm^{-2} was incorporated into the solution. Cyclic voltammograms were recorded in 0.1 M $HClO_4$ electrolyte and in order to remove oxygen a nitrogen purge was applied for 30 min. All the experiments were performed at room temperature. CV data were reported with respect to a normal hydrogen electrode (NHE). Hydrogen oxidation reaction (HOR) activity was determined. By purging the electrolyte solution with oxygen for 30 min, oxygen reduction reaction (ORR) activity was also determined.

Two degradation procedures, namely a) Pt dissolution/agglomeration and b) carbon corrosion, were applied to the prepared catalyst in order to determine the durability of the catalyst.[18]

a) Pt dissolution/agglomeration procedure:

HOR and ORR activities of the catalyst were investigated before and after the Pt degradation test at room temperature. HOR activity was determined for fresh catalyst and the aging of the fresh catalyst was provided by cycling the potential between 0.6 and 1.2 V for 1000 cycles. After the degradation the HOR activity loss was determined by taking into account the electrochemical surface area (ESA) loss. ORR activity was also determined before and after the Pt degradation test.

b) Carbon corrosion procedure:

HOR and ORR activities of the catalyst were investigated before and after the carbon corrosion test at room temperature. HOR activity of the catalyst was obtained both for fresh catalyst and for the aged catalyst

by applying constant 1.2 V potential for 24 h. Electrochemical surface area (ESA) changes before and after the degradation test were determined. ORR activity loss was also determined by applying 1.2 V constant potential to the fresh electrode for 24 h. The voltammograms were obtained in an oxygen saturated electrolyte by rotating the disk electrode between 100 and 2500 rpm at a scan rate of 5 mV s^{-1}. The Tafel slope losses before and after the degradation tests were determined.

4. Conclusions

$ScCO_2$ deposition was used to prepare Pt nanoparticles over PPy/C composite material. The durability of PPy/C composite supported Pt nanoparticles under Pt dissolution/agglomeration and carbon corrosion degradation tests was investigated. $ScCO_2$ deposition resulted in highly dispersed and small Pt nanoparticles over the composite material. Durability tests showed that there was a significant HOR activity loss, which resulted in ESA loss in the catalyst, but insignificant ORR activity was observed with small Tafel slope losses. The durability of the catalyst has to be improved further in order to decrease ESA losses.

Acknowledgments

The authors gratefully acknowledge the financial support from the Scientific and Technological Research Council of Turkey (TÜBİTAK) through grant number 110M081 and Atatürk University BAP projects through grant numbers 2009/256 and 2011/144.

References

1. Saleh, M. H.; Sundararaj, U. *Carbon* **2009**, *47*, 2–22.
2. Shenoy, S. L.; Cohen, D; Weiss, R. A.; Erkey, C. *J. Supercrit. Fluid.* **2004**, *28*, 233–239.
3. Kadırgan, F.; Fıçıcıoğlu, F.; Becerik, İ. *Turk J. Chem.* **1998**, 22, 91–95.
4. Memioğlu, F.; Bayrakçeken, A.; Öznülüer, T.; Ak, M. *Int. J. Energ. Res.* **2014**, *38*, 1278–1287.
5. Rimbu, G. A.; Stamatin, I.; Jackson, C. L.; Scott, K. *J. Optoelectron. Adv. M.* **2006**, *8*, 670–674.
6. Rai, A. R.; Jun, A. P.; Ouajai, W. P.; Ouajai, S. *J. Met. Mat. Min.* **2008**, *18*, 27–31.
7. Wu, T. M.; Chang, H. L.; Lin, Y. W. *Compos. Sci. Techol.* **2009**, *69*, 639–644.
8. Vishnuvardhan, T. K.; Kulkarni, V. R.; Basavaraja, C.; Raghavendra, S. C. *B. Mater. Sci.* **2006**, *29*, 77–83.
9. Zhao, H.; Li, L.; Zhang, Y. *J. Power Sources* **2008**, *184*, 375–380.
10. Chougulea, M. A.; Pawara, S. G.; Godsea, P. R.; Mulika, R. N.; Senb, S.; Patila, V. B. *Soft Nanoscience Letters* **2011**, *1*, 6–10.
11. Garcia, F. L.; Escamilla, G. C.; Flores, A. L.; Tejeda, R. R.; Ordonez, L. C. *Int. J. Electrochem. Sc.* **2013**, *8*, 3794–3813.
12. Memioğlu, F.; Bayrakçeken, A.; Öznülüer, T.; Ak, M. *Int. J. Hydrogen Energ.* **2012**, *37*, 16673–16679.
13. Bayrakçeken, A.; Smirnova, A.; Kitkamthorn, U.; Aindow, M.; Türker, L.; Eroğlu, İ.; Erkey, C. *Chem. Eng. Commun.* **2009**, *196*, 194–203.
14. Yu, X.; Ye, S. *J. Power Sources* **2007**, *172*, 133–144.
15. Witkowska, A.; Greco, G.; Dsoke, S.; Marassi, R.; Cicco, A. *J. Non-Cryst. Solids* **2014**, *401*, 169–174.
16. Lee, K.; Zhang, L.; Lui, H.; Hui, R.; Shi, Z.; Zhang, J. *Electrochim. Acta* **2009**, *54*, 4704–4711.
17. Zhou, Z. M.; Shao, Z. G.; Qin, X. P.; Chen, X. G.; Wei, Z. D.; Yi, B. L. *Int. J. Hydrogen Energ.* **2010**, *35*, 1719–1726.
18. Şayin, E. S.; Bayrakçeken, A.; Eroğlu, İ. *Int. J. Hydrogen Energ.* **2012**, *37*, 16663–16672.
19. Bozkurt, G.; Memioğlu, F.; Bayrakçeken A. *Appl. Surf. Sci.* **2014**, *318*, 223–226.
20. Zhao, H.; Li, L.; Zhang, Y. *J. Power Sources* **2008**, *184*, 375–380.